Dental Materials Journal 2016; 35(2): 309–315

Hardening by cooling rate control and post-firing heat treatment in Pd-Ag-Sn alloy for bonding porcelain

Young-Jun YU[1], Hyo-Joung SEOL[1], Mi-Hyang CHO[2], Hyung-Il KIM[1] and Yong Hoon KWON[1]

[1] *Department of Dental Materials, Institute of Translational Dental Sciences, School of Dentistry, Pusan National University, Beomeo-Ri, Mulgeum-Eup, Yangsan-Si, Gyeongsangnam-Do 626-814, Korea*

[2] *Department of Dental Lab, Wonkwang Health Science University, 344-2 Sinyong-Dong, Jeonbuk, 570-750, Korea*

Corresponding author, Hyo-Joung SEOL; E-mail: seol222@pusan.ac.kr

The aim of this study was to determine the hardening effect by controlling the cooling rate during the porcelain firing process and performing an additional post-firing heat treatment in a Pd-Ag-Sn alloy. The most effective cooling rate for alloy hardening was determined by cooling the specimens at various cooling rates after oxidation treatment. A subsequent porcelain firing simulation followed by cooling at the selected cooling rate was performed. A post-firing heat treatment was then done at 600°C in a porcelain furnace. The hardening mechanism was characterized by a hardness test, X-ray diffraction, field emission scanning electron microscopy and energy dispersive X-ray spectroscopy. Alloy softening occurred during the porcelain firing process followed by cooling at a controlled cooling rate. A post-firing heat treatment allowed apparent precipitation hardening. It is advisable to perform a post-firing heat treatment at 600°C in a porcelain furnace by annealing metal substructure after porcelain fusing.

Keywords: Simulated porcelain firing, Cooling rate control, Post-firing heat treatment, Pd-Ag-Sn alloy for bonding porcelain, Precipitation hardening

INTRODUCTION

When a dental palladium-silver alloy is used to bond the porcelain superstructure, the hardness of the metal substructure is relatively high in the as-cast state. On the other hand, a decrease in hardness often occurs in the metal substructure during the firing process for porcelain fusing[1,2]. Such softening leads to sag and thermal distortion of the metal substructure, resulting in an inaccurate fit of the restoration. In addition, the final hardness of the metal substructure after porcelain firing becomes insufficient to withstand the occlusal force in the oral cavity. Therefore, it is necessary to increase the hardness of dental palladium-silver alloy during and after porcelain firing.

The alloy for bonding porcelain is cooled to room temperature after each firing process to fuse the porcelain. During cooling, the alloy may undergo atomic ordering or precipitation of the components depending on the alloy composition. Therefore, the alloy can be hardened to some extent during cooling[3,4]. In other words, the palladium-silver alloy that was softened during porcelain firing can be hardened by controlling the cooling rate after each firing process. In addition, additional heat treatment can be performed at relatively low temperatures to increase the final hardness of the metal substructure after porcelain fusing. Such post-firing heat treatment can increase the hardness of the metal substructure through atomic ordering or precipitation without melting the porcelain superstructure. The hardening effect by controlling the cooling rate during porcelain firing and an additional post-firing heat treatment has not been reported for dental palladium-silver alloys. The aim of this study was to determine the hardening effects by controlling the cooling rate during the porcelain firing process and an additional post-firing heat treatment in a Pd-Ag-Sn alloy for bonding porcelain and clarifying the hardening mechanism by analyzing the changes in hardness, microstructure, phase transformation, and elemental distribution.

MATERIALS AND METHODS

Specimen alloy

The specimen alloy used in this study was a type IV Pd-Ag-Sn metal-ceramic alloy (Aurolite 1C, Aurium research, USA) with a white color and a fine grain structure. The manufacturer reported that the alloy had a melting range of 1,200–1,270°C and a casting temperature of 1,370°C. The chemical composition of the alloy supplied by the manufacturer was 53.0 wt.% Pd-38.2 wt.% Ag-7.0 wt.% Sn-1.0 wt.% In, with the remainder consisting of Cu, Ru and Zn. Table 1 lists the wt.% and relative at.% that was calculated by taking the total wt.% of all components except for Cu, Ru and Zn as 100 wt.%. To simulate complete porcelain firing, the specimens were cast using the lost wax casting technique in a vacuum casting machine (Combilabor CL-G 94, Heraeus Kulzer, Germany). All castings were bench-cooled to room temperature, followed by divesting. The specimens obtained were in the form of small square pieces, 10×10×1.2 mm^3 in size.

Isothermal age-hardening heat treatment

To identify the isothermal age-hardening mechanism of the alloy, the as-received specimens were solution-treated at 1,000°C for 10 min followed by quenching

Received May 28, 2015: Accepted Nov 24, 2015
doi:10.4012/dmj.2015-189 JOI JST.JSTAGE/dmj/2015-189

Table 1 Chemical composition of the specimen

Composition	Pd	Ag	Sn	In	Cu	Ru	Zn
wt.%	53.00	38.20	7.00	1.00	<1	<1	<1
at.%	54.14	38.50	6.41	0.95	—	—	—

Table 2 Simulated porcelain firing cycle

Firing stage	Pre-drying (min)	Heat rate (°C/min)	Final temp. (°C)	Time at final temp. (min)	Vacuum time (min)
Oxidation	0	60	1,040	10	0
1st opaque	2	60	970	1	6:10
2nd opaque	2	60	960	1	6:00
Main bake	5	60	940	1	5:40
Correction	5	60	910	1	5:10
Glaze	2	60	900	0	5:00
Glaze only	2	60	900	0	5:00

Table 3 Cooling rate during simulated firing

Cooling rate	Ice quenching	Stage 0	Stage 1	Stage 2	Stage 3
Condition	quenching into ice brine	firing chamber moves immediately to upper end position	firing chamber opens about 70 mm	firing chamber opens about 50 mm	firing chamber remains closed

into ice brine, isothermal aging at 500°C in a molten salt bath for various time periods until 20,000 min and quenching into ice brine.

Cooling rate control during porcelain firing simulation and post-firing heat treatment

To select the most effective cooling rate for alloy hardening, the as-cast specimens were oxidation treated at 1,040°C for 10 min, cooled to 600°C at various cooling rates in a porcelain furnace (Multimat 2 touch, Dentsply, Germany) and then bench cooled to room temperature. The oxidation treatment is the first stage of the simulated porcelain firing cycle presented in Table 2. Table 3 lists the various cooling rates in the order of rapidity. A subsequent porcelain firing simulation followed by cooling at the selected cooling rate was performed according to Table 2. An additional post-firing heat treatment was then conducted in a porcelain furnace (Multimat 2 touch, Dentsply) that had been adjusted to 600°C and then bench cooled to room temperature.

Hardness test

Hardness measurements were completed for the porcelain firing simulated and post-firing heat treated specimens using a Vickers micro-hardness tester (MVK-H1, Akashi, Japan) at 300 gf with a dwell time of 10 s. All hardness results were recorded as the mean values of five measurements.

Field emission scanning electron microscopy (FE-SEM)

The isothermally aged specimen at 500°C, the porcelain firing simulated and post-firing heat treated specimens were prepared using a standard metallographic technique for the FE-SEM observations (JSM-6700F, Jeol, Japan). Subsequently, a freshly prepared aqueous solution of 10% potassium cyanide (KCN) and 10% ammonium persulfate ($(NH_4)_2S_2O_8$) was used for final etching of the specimens. The specimens were examined by FE-SEM at 15 kV.

X-ray diffraction (XRD) study

To identify the isothermal age-hardening mechanism of the alloy, the changes in the XRD pattern during isothermal aging at 500°C were examined from powder specimens that had been passed through a 330 mesh screen after filing the plate-like samples. After being vacuum-sealed in a silica tube and solution-treated

at 1,000°C for 10 min, followed by quenching in ice brine, the powder specimens were aged isothermally at 500°C in a molten salt bath until 20,000 min, and then quenched in ice brine.

The porcelain firing simulated and post-firing heat treated plate specimens were prepared using a standard metallographic technique for XRD (XPERT-PRO, Philips, The Netherlands). The XRD profile was recorded at 40 kV and 30 mA using nickel-filtered Cu Kα radiation as the incident beam. The scan rate of the goniometer was 1° (2θ/min).

Energy dispersive spectrometry (EDS) analysis

The changes in the elemental distribution of the porcelain firing simulated and then post-firing heat treated specimen were examined by EDS (INCA x-sight, Oxford Instruments, UK) at 15 kV that was attached to the FE-SEM.

RESULTS

Isothermal age-hardening mechanism

The specimens show the apparent age-hardenability during isothermal aging at 500°C after solution-treatment at 1,000°C for 10 min (Fig. 1). The changes in the microstructure and XRD pattern during isothermal aging at 500°C revealed the isothermal age-hardening to be due to the precipitation of a face-centered tetragonal (f.c.t) β phase with lattice parameters of a_{100}=4.047 Å and c_{202}=3.757 Å from a face-centered cubic (f.c.c.) α phase with a lattice parameter of a_{200}=3.9778 Å (Figs. 2 and 3). Therefore, the specimen alloy was expected to undergo precipitation hardening during cooling after porcelain firing at approximately 1,000°C.

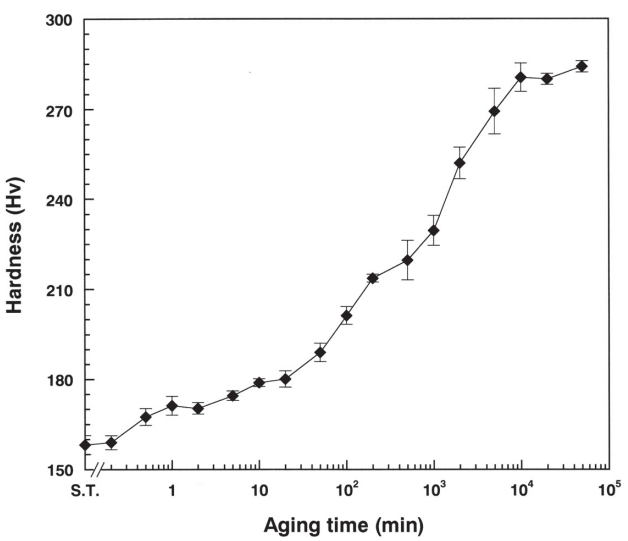

Fig. 1 Changes in the hardness during isothermal aging at 500°C (S.T.: solution-treated specimen).

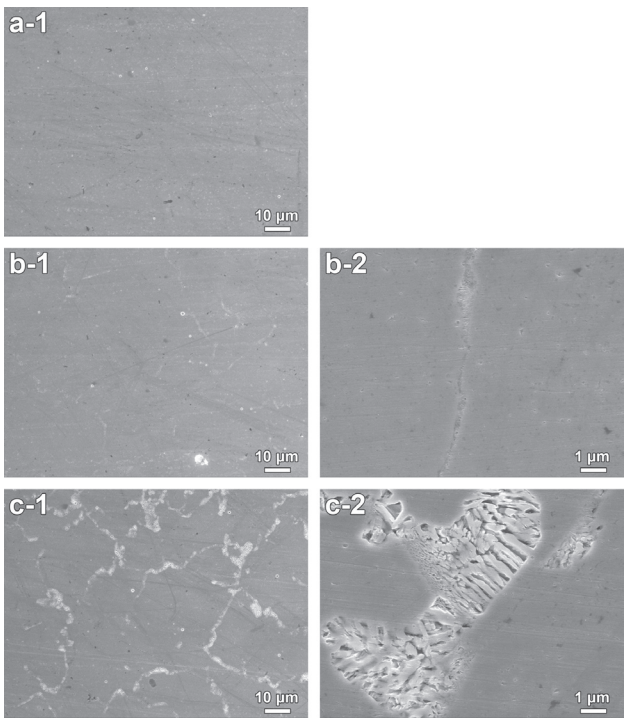

Fig. 2 Changes in the microstructure during isothermal aging at 500°C: solution-treated specimen (a), 100 min (b), 10,000 min (c) at magnifications of ×1,000 (1) and ×10,000 (2).

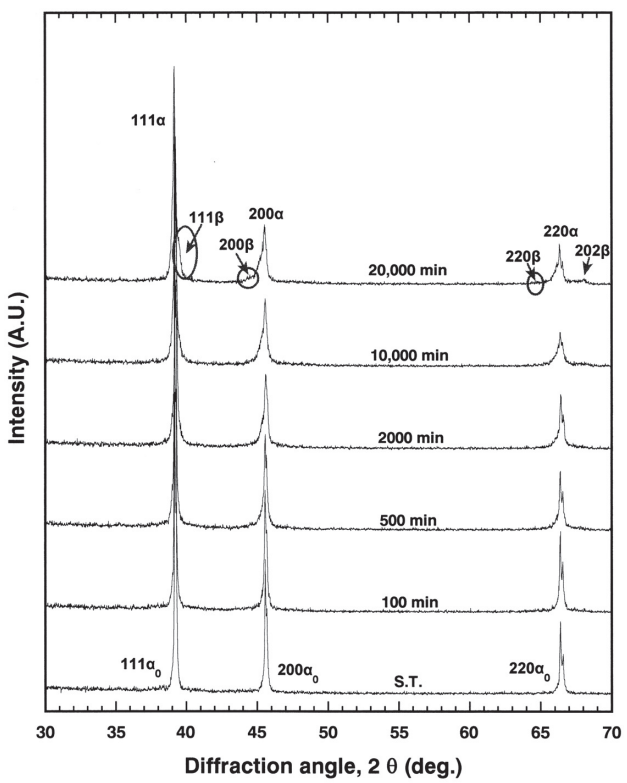

Fig. 3 Changes in the XRD pattern during isothermal aging at 500°C (S.T.: solution-treated specimen).

Table 4 Hardness at each cooling rate during simulated oxidation treatment

Cooling rate	Ice quenching	Stage 0	Stage 1	Stage 2	Stage 3
Hardness (HV)	151.7 (±2.01)	167.8 (±0.45)	168.1 (±2.46)	176.7 (±1.40)	168.1 (±2.11)

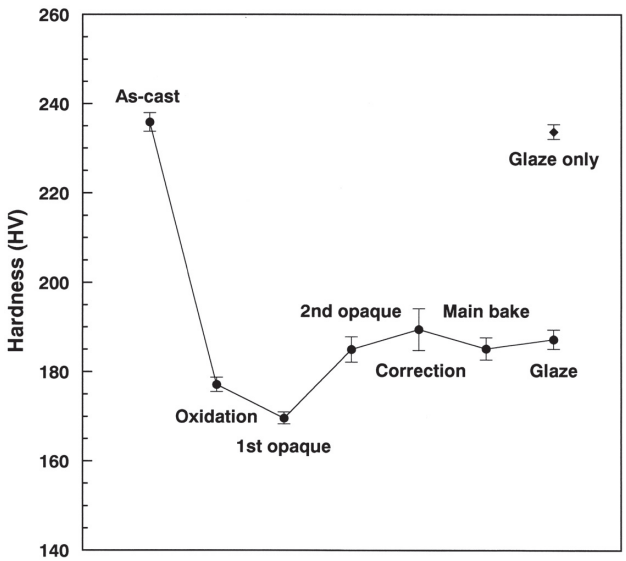

Fig. 4 Hardness changes in the as-cast specimen during simulated porcelain firing.

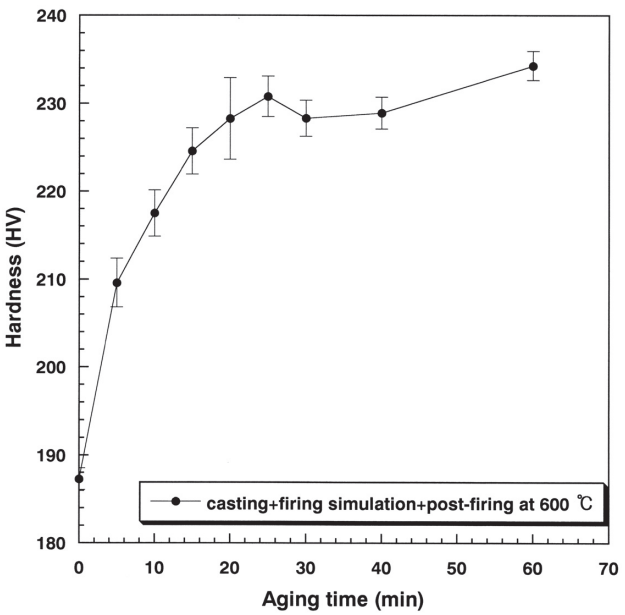

Fig. 5 Hardness changes in the as-cast and then firing simulated specimen during post-firing heat treatment at 600°C.

Hardness changes at various cooling rates during porcelain firing simulation

The most effective cooling rate for precipitation hardening of the alloy was selected by cooling the specimens at various cooling rates after the oxidation treatment. Table 4 lists the obtained hardness at each cooling rate. The specimen cooled by ice quenching showed the lowest hardness (151.7 HV). The hardness increased slightly as the cooling rate was decreased from stage 0 to stage 2. In stage 3, the hardness decreased again. Hence, stage 2 (firing chamber opened approximately 50 mm), which is the intermediate rate, was most effective in hardening the alloy even though the hardening effect was not great.

Hardness changes by simulated porcelain firing at controlled cooling rate and post-firing heat treatment

Figure 4 shows the changes in hardness during simulated porcelain firing followed by cooling at a controlled cooling rate. The cooling rate was set to stage 2 in each firing cycle. The hardness was 235.9 HV in the as-cast state, which then decreased from the first stage of the simulated porcelain firing cycle (oxidation). A low hardness was maintained during subsequent firing until the final firing stage, glazing (187 HV). In contrast, the high hardness of the as-cast condition was maintained (233.7 HV) in the specimen treated with only glazing at 900°C without an intermediate firing process.

Figure 5 shows the changes in hardness by the post-firing heat treatment at 600°C. The hardness of the post-firing heat treated specimen increased from 187 to 230 HV within 25 min. After that, the high hardness value was maintained until 60 min.

Changes in microstructure

The as-cast specimen exhibited an equiaxed structure, and acicula or particle-like precipitates were observed adjacent to the grain boundary (Fig. 6-a). In the oxidation-treated specimen at 1,040°C, the precipitate adjacent to the grain boundary disappeared and fine-grain interior precipitates were observed in the matrix (Fig. 6-b). This homogenized microstructure did not change in the subsequent firing cycles until the main bake (Fig. 6-c) and glaze (Fig. 6-d). On the other hand, in the glaze-only specimen without intermediate firing (Fig. 6-e), the microstructure was similar to those of the as-cast specimen without homogenization. By a post-firing heat treatment at 600°C for 60 min (Fig. 6-f), lamellar structures appeared at the grain boundaries, and particle-like precipitates in the grain interior became more apparent than those before the post-firing heat treatment, as shown in Fig. 6-d.

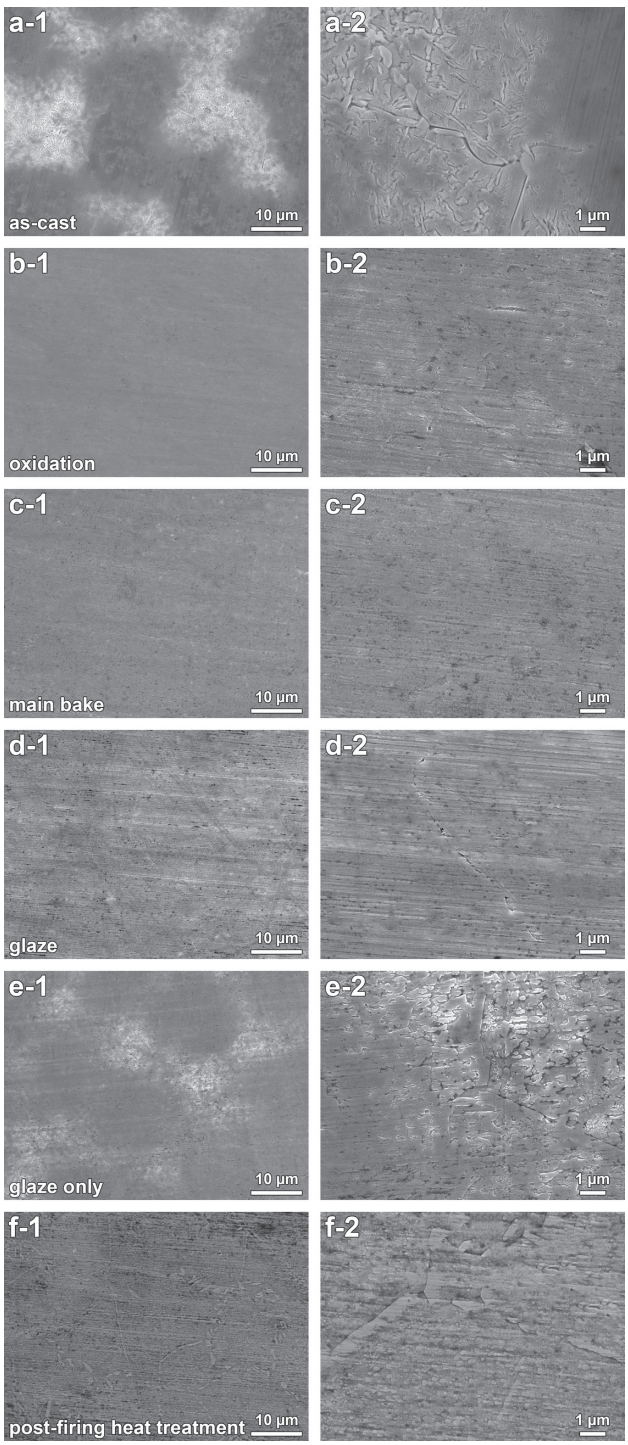

Fig. 6 Microstructural changes in the as-cast specimen during simulated porcelain firing and post-firing heat treatment at 600°C: as-cast (a), oxidation (b), main bake (c), glaze (d), glaze only (e), post-firing heat treatment at 600°C for 60 min (f) at magnifications of ×2,000 (1) and ×10,000 (2).

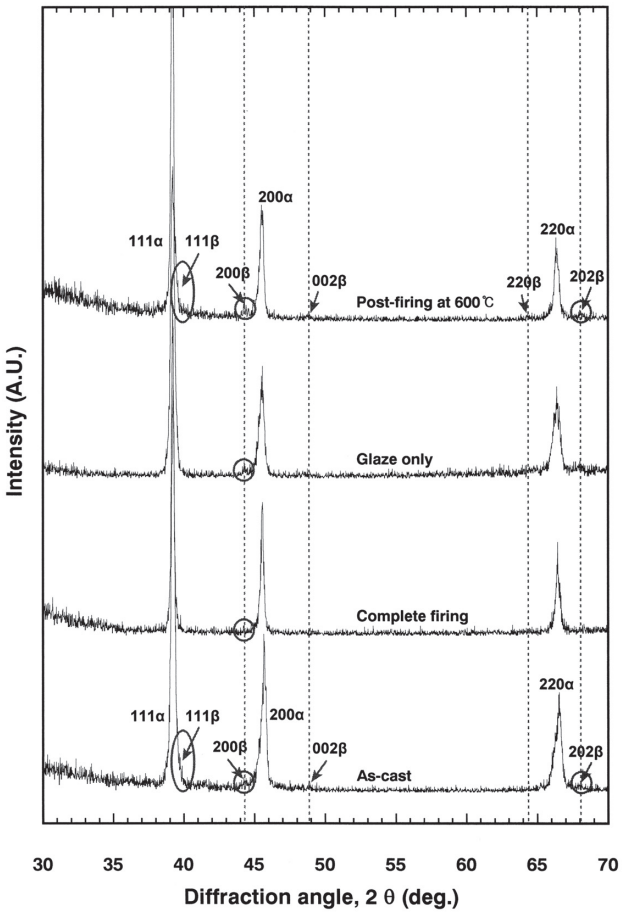

Fig. 7 Changes in the XRD patterns of the as-cast specimen after simulated porcelain firing and post-firing heat treatment at 600°C.

Changes in crystal structure

The changes in the XRD patterns by the simulated porcelain firing and post-firing heat treatment were observed (Fig. 7). In the as-cast specimen, a f.c.c. phase with a lattice parameter of a_{200}=3.9828 Å was the main phase (the α phase), and a f.c.t phase with the lattice parameters, a_{200}=4.0866 Å and c_{002}=3.7257 Å, was the minor phase (the β phase). Therefore, the matrix is composed of a f.c.c. α phase and the precipitates are composed of a f.c.t β phase. By the porcelain firing process, the peak intensity of the β precipitates decreased, supporting microstructural homogenization. In the glaze-only specimen without an intermediate firing process, however, the peak intensity of the β precipitates did not become weak. In the specimen post-firing heat treated at 600°C after complete firing, the peak intensity of the β precipitates became strong again, indicating that the precipitation had occurred.

Elemental analysis

Figure 8 presents an FE-SEM image of the specimen that underwent porcelain firing followed by post-firing heat

Table 5 EDS analysis at the regions marked in Fig. 8

at.%	Pd	Ag	Sn	In	Cu	Ru	Zn
M1	51.35	45.72	2.93	0	0	0	0
M2	55.19	40.33	4.48	0	0	0	0
P1	73.70	9.99	16.31	0	0	0	0
P2	72.27	14.32	13.41	0	0	0	0

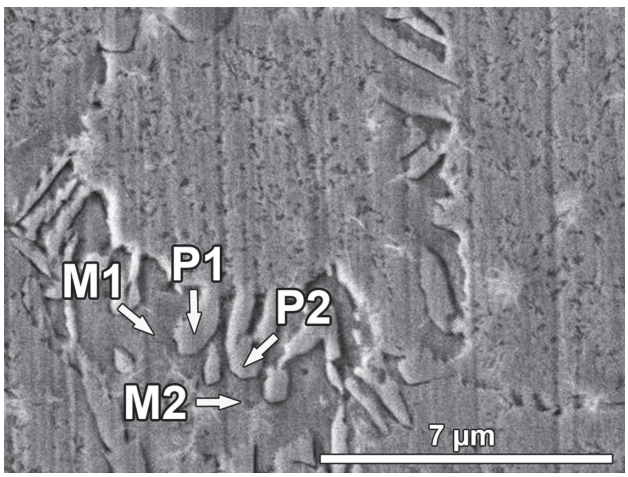

Fig. 8 FE-SEM image of the post-firing heat treated specimen at 600°C for 60 min for EDS analysis (M, matrix; P, precipitate at a magnification of ×6,000).

treatment at 600°C for 60 min. Table 5 lists the results of EDS point analysis for each region marked with an arrow in Fig. 8. In the matrix (M), the Pd and Sn content decreased and the Ag content increased compared to the alloy composition in Table 1. In the precipitate (P), the content of Ag decreased, and Pd and Sn increased compared to the alloy composition. No In, Cu, Ru, or Zn was detected due to their minor contents.

DISCUSSION

Dental alloys for bonding porcelain are used to fabricate the substructure of a porcelain superstructure in metal-ceramic prostheses. Therefore, the alloys are cast in a very thin shape to prevent a decrease in the aesthetic potential of the semi-translucent outer layer made of porcelain. The thin cast undergoes heat treatment several times during firing of the porcelain superstructure. When dental gold alloy is used to bond porcelain, the mechanical properties, such as hardness, are poor in the as-cast state. This is related to the poor sag resistance of the metal substructure when the porcelain is fired at approximately 1,000°C, which causes serious problems, such as an inaccurate fit of the restoration[5,6]. Therefore, several studies of the heat treatment of dental gold alloys for bonding porcelain have been performed to improve the hardness before firing porcelain on the alloy[3,7-10].

For dental palladium-silver alloys used for bonding porcelain, the hardness of the metal substructure is relatively high in the as-cast state. On the other hand, the porcelain firing process often causes softening of the metal substructure[1,2], resulting in insufficient mechanical properties of the final prosthesis to withstand the occlusal force in addition to sag and thermal distortion of the metal substructure during porcelain firing. Little experimental data is available on improving the hardness of dental palladium-silver alloy for bonding porcelain during and after the porcelain firing process.

In this study, from the changes in the hardness, microstructure and XRD pattern during isothermal aging at 500°C (Figs. 1–3), the Pd-Ag-Sn alloy was expected to be hardened by precipitation during cooling after porcelain firing at approximately 1,000°C. Therefore, to select the most effective cooling rate for alloy hardening, the specimens were cooled at various cooling rates after the oxidation treatment, which is the first stage of the simulated porcelain firing cycle. As a result, the oxidation-treated specimens after casting showed lower hardness than the as-cast specimen at all cooling rates (Table 4). The specimen cooled by ice quenching showed the lowest hardness of 151.7 HV, which is similar to that of the solution treated specimen at 1,000°C for 10 min (158 HV). Therefore, the specimen is believed to be solutionized during the oxidation treatment. As the cooling rate decreased, the hardness increased slightly. At the slowest cooling rate (stage 3), however, the hardness decreased. Therefore, precipitation hardening was confirmed to occur during cooling, where the cooling rates affect the hardening efficiency. This trend was also reported for the CuPt alloy, where effective order hardening occurred during cooling at an intermediate cooling rate, and a slower cooling rate induced softening by domain growth[11].

The decreased hardness after the oxidation treatment was not recovered during the subsequent porcelain firing process followed by cooling at an intermediate cooling rate (Fig. 4). The final hardness after the complete firing simulation was 187 HV, which is insufficient for the metal substructure to withstand the occlusal forces in the oral cavity. In the Pd-Ag-Sn alloy examined, precipitation hardening occurred

during isothermal age-hardening heat treatment at 500°C (Figs. 1–3). Therefore, heat treatment at relatively low temperatures after porcelain fusing is believed to strengthen the softened metal substructure without melting the porcelain superstructure. On the other hand, the increasing rate in hardness was too slow at 500°C (Fig. 1), which makes the process time consuming. Therefore, to make atomic diffusion faster, the temperature for post-firing heat treatment was increased to 600°C[12]. As a result, the hardness of the post-firing heat treated specimen increased from 187 to 230 HV within 25 min, and the high hardness value was maintained until 60 min (Fig. 5). The prolonged post-firing heat treatment, however, was believed to cause softening due to over aging[13,14].

The microstructural changes showed that softening by the oxidation treatment resulted from microstructural homogenization, and the homogenized microstructure was maintained until the final firing stage (Fig. 6). Softening by microstructural homogenization after complete porcelain firing was also reported in a Pd-Ag alloy (60Pd-28Ag-6Sn-5In with minor Ga and Ru) with a higher Pd content[1,15]. On the other hand, after the post-firing heat treatment at 600°C for 60 min, lamellar structures appeared at the grain boundaries, and particle-like precipitates in the grain interior became more apparent than those before the post-firing heat treatment. Therefore, the hardening effect obtained by the post-firing heat treatment was caused by precipitation of the alloying elements from the matrix. Such a result was supported by XRD (Fig. 7), which showed that the post-firing heat treatment allowed precipitation effectively in the homogenized specimen after porcelain firing simulation. The precipitates were concentrated with Pd and Sn. Therefore, by considering the EDS result together with the XRD study, the β precipitates were composed of the Pd_3Sn-based phase with a f.c.t structure, and the α matrix was composed of the Pd-Ag-rich phase with a f.c.c structure. The precipitation of the f.c.t β phase from the f.c.c. α matrix must have produced large lattice strain in the matrix due to the difference in the lattice parameters between the matrix and precipitates, resulting in apparent hardening[1,13,16].

CONCLUSION

These results showed that the alloy softened during the porcelain firing process followed by cooling at a controlled cooling rate. A post-firing heat treatment at 600°C allowed apparent alloy hardening induced by precipitation. In conclusion, for practical work on Pd-Ag-Sn alloys, post-firing heat treatment by annealing the metal substructure at 600°C for 25 min in the porcelain furnace after porcelain fusing is recommended to increase the hardness of the metal substructure that had been softened during porcelain firing.

ACKNOWLEDGMENTS

This research was supported by the Basic Science Research Program through the National Research Foundation of Korea (NRF), funded by the Ministry of Education, Science and Technology (grant number: NRF-2014R1A1A2055018).

REFERENCES

1) Guo WH, Brantley WA, Clark WAT, Monaghan P, Mills MJ. Transmission electron microscopic investigation of a Pd-Ag-In-Sn dental alloy. Biomaterials 2003; 24: 1705-1712.
2) Li D, Baba N, Brantley WA, Alapati SB, Heshmati RH, Daehn GS. Study of Pd-Ag dental alloys: examination of effect of casting porosity on fatigue behaviour and microstructural analysis. J Mater Sci Mater Med 2010; 21: 2723-2731.
3) Fischer J, Fleetwood PW. Improving the processing of high-gold metal-ceramic frameworks by a pre-firing heat treatment. Dent Mater 2000; 16: 109-113.
4) German RM. Hardening reactions in a high-gold content ceramo-metal alloy. J Dent Res 1980; 59: 1960-1965.
5) Tuccillo JJ, Nielsen JP. Creep and sag properties of a porcelain-gold alloy. J Dent Res 1967; 46: 579-583.
6) Iwashita H, Kuriki H, Hasuo T, Ishikawa K, Hashimoto K. Studies on dimensional accuracy of porcelain fused to precious metal crown. The influence of the porcelain to the metal coping on porcelain fusing procedure. Shigaku 1977; 65: 110-125.
7) Jeon BW, Kim SM, Kim HI, Kwon YH, Seol HJ. Hardening effect of pre-and post-firing heat treatment for a firing-simulated Au-Pd-In metal-ceramic alloy. Gold Bull 2014; 47: 255-261.
8) Wang JN, Liu WB. A Pd-free high gold dental alloy for porcelain bonding. Gold Bull 2006; 39: 114-120.
9) Ito M, Kikuchi M, Okuno O, Kimura K. Ceramic bonding strength of Au-1.6 wt% Ti alloy. Dent Mater J 2005; 24: 268-274.
10) Liu WB, Wang JN. Strengthening of a Pd-free high gold dental alloy for porcelain bonding by a pre-firing heat treatment. Dent Mater 2007; 23: 1136-1141.
11) Hisatsune K, Ohta M, Yamane M. Effect of cooling rate on ordering behaviour in a CuPt alloy. Dent Mater J 1982; 1: 1-7.
12) Seol HJ, Kim GC, Son KH, Kwon YH, Kim HI. Hardening mechanism of an Ag-Pd-Cu-Au dental casting alloy. J Alloys Compd 2005; 387: 139-146.
13) Hisatsune K, Hasaka M, Sosrosoedirdjo BI, Udoh K. Age-hardening behaviour in a palladium-base dental porcelain-fused alloy. Mater Charact 1990; 25: 177-184.
14) Payan J, Moya GE, Meyer JM, Moya F. Changes in physical and chemical properties of a dental palladium-silver alloy during metal-porcelain bonding. J Oral Rehabil 1986; 13: 329-338.
15) Guo WH, Brantley WA, Li D, Clark WAT, Monaghan P, Heshmati RH. Annealing study of palladium-silver dental alloys: Vickers hardness measurements and SEM microstructural observations. J Mater Sci Mater Med 2007; 18: 111-118.
16) Hisatsune K, Udoh K, Nakagawa M, Yasuda K. Three distinguishable phase changes during slow-cooling in commercial dental alloys for porcelain bonding. Dent Mater J 1987; 6: 54-63.